D1.2 | Spin filtering tunnel barriers

Author(s): Max Ilyn, Sebastian Bergeret, Celia Rogero

Delivery date: 25.02.2021
Version: 1.0

This project has received funding from the European Union's Horizon 2020 research and innovation programme under grant agreement No 800923.

Project Acronym:	SUPERTED
Project Full Title:	Thermoelectric detector based on superconductor-ferromagnet heterostructures
Call:	H2020-FETOPEN-2016-2017
Topic:	FETOPEN-01-2016-2017
Type of Action:	RIA
Grant Number:	800923
Project URL:	https://superted-project.eu/

Editor:	Maxim Ilyn, Celia Rogero, Sebastian Bergeret CSIC, Tero Heikkilä (JYU)
Deliverable nature:	Report (R)
Dissemination level:	Public (PU)
Contractual Delivery Date:	28.02.2021
Actual Delivery Date:	25.02.2021
Number of pages:	14
Keywords:	tunnel junctions, spin-splitting
Author(s):	Maxim Ilyn, CFM-CSIC Celia Rogero, CFM-CSIC
Contributor(s):	Carmen González Orellana, CFM-MPC foundation Elia Strambini, CNR Maria Spies, CNR Sebastian Bergeret, CFM-CSIC Mikel Rouco CFM-CSIC Alberto Hijano CFM-MPC foundation Stefan Ilic CFM-CSIC Subrata Chakraborty, JYU Faluke Aikebaier, JYU Pauli Virtanen, JYU Tero Heikkilä, JYU Sanna Rauhamäki, JYU
External contributor(s):	Sara Khorshidian, CNR Vitaly Golovach, DIPC

Abstract

This deliverable 1.2 is the report of the mid project results regarding the growth and fabrication of the ferromagnet/superconductor (FI/S) multilayer devices. In particular, the report includes the results and evaluation of the spin-filtering tunnel barriers we have been focused on as well as the chosen material combination, preparation and characterization.

This project has received funding from the European Union's Horizon 2020 research and innovation programme under grant agreement No 800923.

1. Introduction

In the framework of the development of a novel thermoelectric detector, important efforts are focused on the growth and patterning of the multilayer thin-film junctions containing ferromagnetic insulators and superconducting materials. The primary goal reported in a previous deliverable document (D1.1) was the development of the process suitable for the growth of Al/EuS bilayers with tunable strength of exchange coupling and fabrication of the devices. Our next step within the development of the project is achieving of the spin-split Density of States (DOS) of the superconducting layer, ideally at zero applied field, and demonstration of spin-dependent asymmetry of the tunneling current. Both spin splitting and spin-dependent tunneling are essential requirements for the SUPERTED detector. In this deliverable we report on the successful demonstration of both effects in $Al/AlO_x/Al/EuS$ and $Co/AlO_x/Al/EuS$ tunnel junctions and describe additional activity aimed to exploration of the alternative materials suitable for making spin-filtering magnetic tunnel barriers.

This is the **first demonstration** of the **measured spin splitting of the superconducting density of states at zero field** in samples produced by someone else than the pioneer in the field, J. Moodera at MIT, the USA. It therefore fulfills the first general goal of SUPERTED: *Developing a fabrication process and setting a European fabrication facility* that will allow building devices composed of nanoscale ferromagnetic insulator/superconductor (FI/S) bilayers with an optimized magnetic proximity effect in S.

This project has received funding from the European Union's Horizon 2020 research and innovation programme under grant agreement No 800923.

2. Demonstration of the exchange-split DOS in the tunnel junctions Al/AlO_x/Al/EuS and Co/AlO_x/Al/EuS

The superconducting thermoelectric element we are aiming at consists of a tunnel junction that features a Spin-Polarized Tunneling (SPT) current and has one of its electrodes made of a superconducting material (S) that features a spin-split DOS of the quasi particles close to the Fermi level. SPT is provided either by a spin-polarized ferromagnetic (FM) counter electrode or by so-called spin-filtering barrier, which is a tunnel barrier that creates non-equal probability of tunneling for the electrons with different orientations of spins. On the other hand, a spin-split DOS of the S electrode hast to be created via exchange coupling to the adjacent Ferromagnetic Insulating (FI) layer in order to avoid using large external magnetic fields

Growth of S/FI double-layered thin films with tunable exchange coupling turned out to be a serious challenge for materials scientists. To date, best performing bilayer Al/EuS of acceptable quality was demonstrated only by the group of Dr. Moodera at MIT, meanwhile other attempts to reproduce his results ended up in the samples that needed in some external magnetic field to create the exchange-split DOS [1]. Therefore, the main objective of the work package one of the SuperTED project was a development of the growth technique capable of producing the Al/EuS bilayers with suitable exchange coupling strength and a clear spin-split DOS even at zero applied field. The work of the experimental part of the CSIC group during the first year of the project was aimed to investigation of the properties of the EuS thin films and Al/EuS bilayers [2]. In parallel, the upgrade of the experimental setup had been performed to append a shadow mask patterning capability in order to start making in situ the Al/EuS-based tunnel junctions in the UHV research chamber [2]. With the help of developed theoretical modelling of the spectral properties of S/FI bilayer [3] we deeply understood our experimental findings and develop during a second year of the project a recipe of growth of the Al/EuS bilayers with spin-split DOS.

According to the theory, the parameters that affect the DOS at the outer interface of the Al-film in the Al/EuS bilayer are the thickness of the Al film, the effective exchange coupling field $\overline{h}$ and the spin-flip relaxation rate τ_{sf} [3]. Our experiments have demonstrated that these latter two parameters strongly depend on the morphology and stoichiometry of the EuS layer. A series of Al/AlO_x/Al/EuS tunnel junctions with different thicknesses of the exchange-coupled bottom aluminum layer and variable magnitude of $\overline{h}$ was made to demonstrate these trends. Table 1 summarizes main properties of these samples. When the thickness of the bottom Al is bigger than the critical value, the tunneling conductance dI/dV of the junctions measured at temperatures below the superconducting transition point has characteristic shape with two split peaks of the BCS density of states separated by a gap with zero conductance (see Fig.1 (b)). In contrary, if the thickness of the Al is lower than the critical value, the bottom layer remains non-superconducting down to 30 mK and respective dI/dV curve shows no splitting (not shown). It is worth mentioning that the critical thickness of the superconducting layer depends on the strength of the exchange coupling [3] (see also Table 1).

This project has received funding from the European Union's Horizon 2020 research and innovation programme under grant agreement No 800923.

Once the interaction on the S/FI interface is close to the Chandrasekhar-Clogston limit, the external field is capable of quenching the superconductivity as it was found, for example, in the case of the sample S3 (see Fig.1 (a-b)). It is worth to emphasize that our superconducting samples show a clear spin-splitting in the DOS (Fig. 1a) even at zero applied magnetic field. This is a remarkable achievement having in mind that until now spin splitting at zero field had only been observed in the samples fabricated by Moodera at MIT.

Tuning of the exchange coupling strength to this pre-critical value allowed us to demonstrate the influence of the morphology of the EuS film on the magnitude of the S-FI interaction. Magnetic properties of the thin films of EuS were studied in several works. To check the consistency of our data, we have grown a 12 nm thick film of EuS on the polished fused silica substrate under the same conditions that were used for the fabrication of the tunnel junctions.

Table 1: *Properties of the Al layer in contact with the EuS for Al/AlOx/Al/EuS tunnel junctions. The averaged exchange field is extracted from the data at zero magnetic field. The last column gives the critical thickness obtained from the model.*

Sample	d (nm)	$\Delta_{2,0}$ (μeV)	$\bar{h}$ (μeV)	d_c (nm)
S1	10	245	78.5	4.5
S2	8	255	118.5	5.3
S3	9	245	146	7.6
S4	3	0	No SC	5.4

Figure 2(a) shows the magnetization loop measured at 5 K in the magnetic field applied parallel to the film. Magnetization reversal occurs at the coercive field of 2.4 mT. The film has a large value of the remanent magnetization similar to what was observed for the samples of Moodera's group [4]. Nevertheless, magnetization grows slowly and saturates only in the field of a few Tesla. It implies that a polycrystalline EuS includes a certain amount of superparamagnetic grains weakly coupled to the main film. Relatively small value of the coercive field corroborates this observation. Indeed, for the magnetization reversal dominated by the domain walls movement, the coercive field increases with the increasing size of the magnetic irregularities

This project has received funding from the European Union's Horizon 2020 research and innovation programme under grant agreement No 800923.

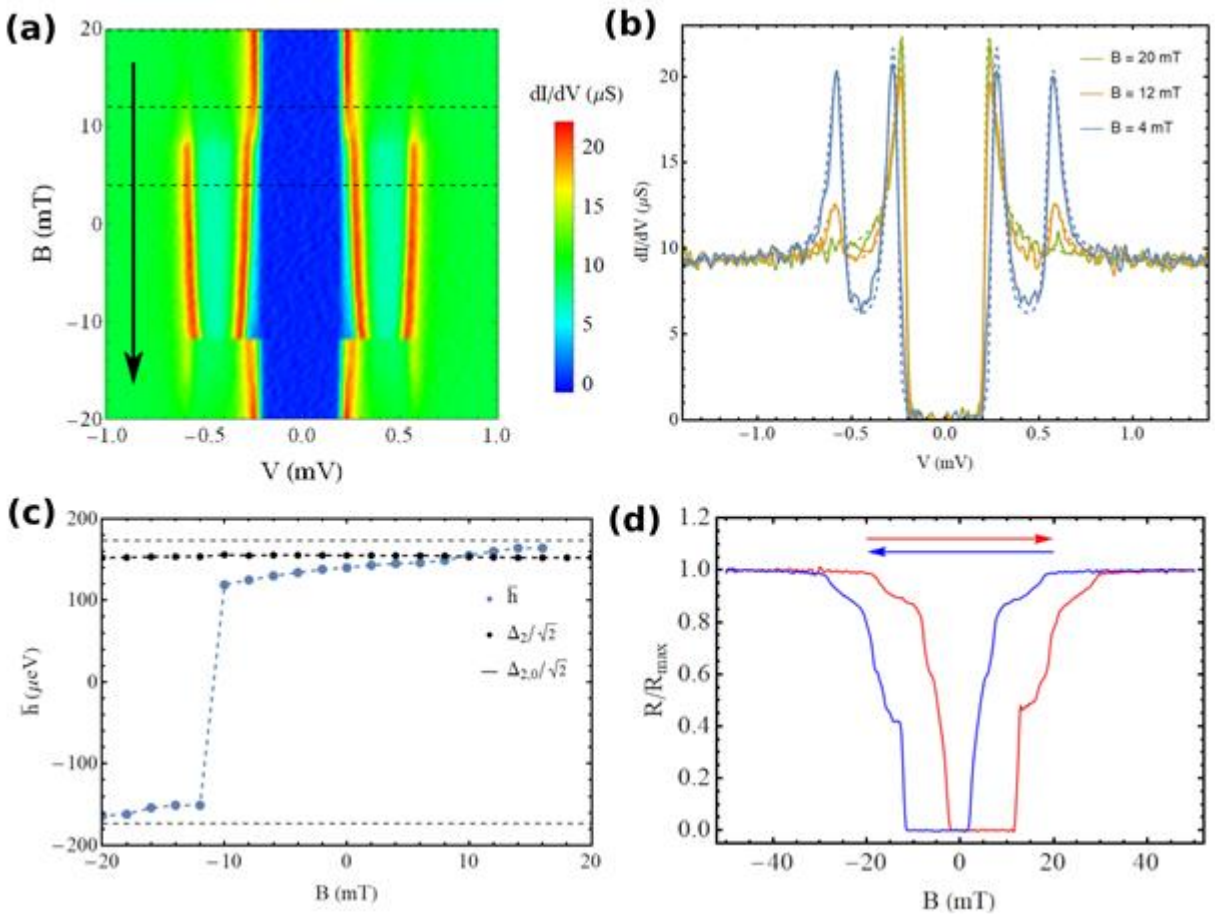

Figure 1: *(a) Differential conductance of the S3 sample measured at 30 mK as a function of the external magnetic field and the voltage drop across the junction. The arrow indicates the direction of the magnetic field sweep. At B = 10 mT most of the bottom Al film undergoes a transition into the superconducting state. (b) dI/dV curves at three different values of B (B = 4, B = 12 and B = 20 mT), indicated by dashed lines in (a). The solid lines correspond to the experimental data, whereas the dashed lines to the theoretical fitting. The values of the fitting parameters used in the theoretical model at B = 0 are* $\bar{h}$ *= 146 μeV,* Δ_2 *= 219 μeV and* τ_{sf}^{-1} *= 38.5 μeV. (c) Effective exchange field,* $\bar{h}$*, and self-consistent order parameter,* Δ_2 *of the bottom Al layer divided by* $\sqrt{2}$*. The horizontal dashed lines represent the Chandrasekhar-Clogston critical field* $\Delta_{2,0}/\sqrt{2}$ *in the absence of magnetic impurities. (d) Magnetoresistance of the bottom Al film adjacent to the EuS layer measured at T = 30 mK.*

This project has received funding from the European Union's Horizon 2020 research and innovation programme under grant agreement No 800923.

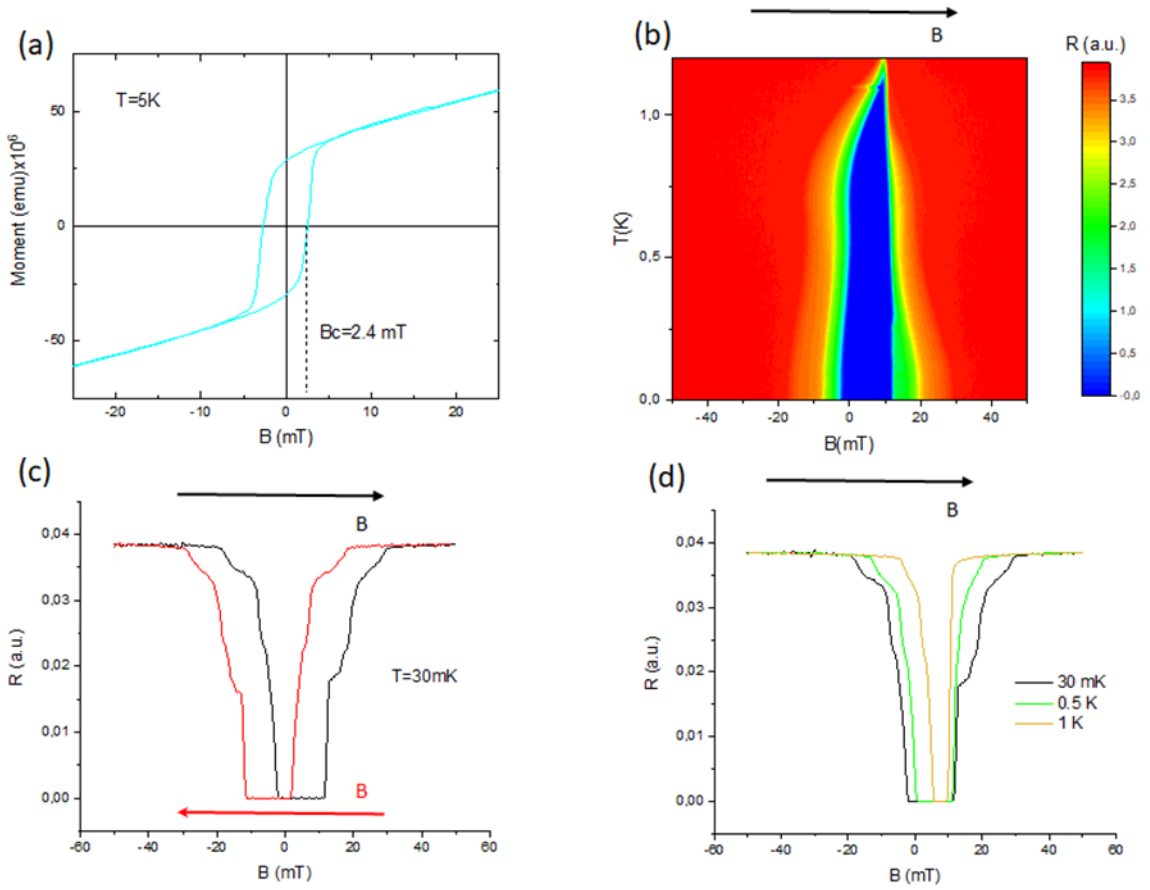

Figure 2: *(a) Magnetization loop measured for a continuous EuS film at 5 K, with the field applied in the in-plane direction. (b) Contour plot showing the resistance of Al wire adjacent to the EuS layer as a function of the external field and the temperature. The arrow indicates direction of the magnetic field. These measurements and the measurements shown in the next two panels were performed on the sample S3. (c) The hysteresis of the resistance of the Al wire adjacent to the EuS layer at T = 30 mK. (d) The B-field dependence of the resistance of the Al wire adjacent to the EuS layer at different temperatures.*

Therefore, fine polycrystalline structure results in lower coercive fields [4]. Comparing the magnetization loop presented in Fig. 2(a) with the data reported in Ref. [4], it is clear that the coercive field in our sample is similar to the coercive field of thin EuS films grown at 77 K which were found to have grains with diameters about 4.4 nm. Since EuS has no magnetocrystalline anisotropy, it is reasonable to expect very low values of the blocking temperature for the small superparamagnetic grains [5].

We could not measure magnetization loops below 2 K. However, the dependence of the bottom Al layer's resistance interfaced with EuS film on the magnetic field provides indirect confirmation of this conjecture [3]. At 30 mK, all superparamagnetic particles are supposed to be in the blocked state. Respective $R(B)$-curve shows distinctive jumps that can be interpreted as magnetization reversal of the components with different magnetic anisotropy (Fig. 2(c)). If the exchange coupling between the grains is weak, the orientation of their magnetic moments depends on the dipolar interaction with the rest of the film and on the Zeeman interaction with the external field. Whereas the external field will try to

This project has received funding from the European Union's Horizon 2020 research and innovation programme under grant agreement No 800923.

align the particles' moment, the dipolar interaction tries to orient the moment of the particles in the direction opposite to the magnetic moment of the film. Considering a descending branch of the resistance (red curve in Fig. 2(c)), we can see that all moments are aligned at a high positive field, and the effective exchange field is high (no superconductivity). When the field decreases down to zero, the dipolar interaction dominates. The resistance decreases in steps that correspond to consecutive switching of the magnetization of the superparamagnetic particles. The average magnetic moment becomes smaller and leads to a decrease in the effective exchange field. This decrease allows the Al wire to become superconducting. The zero-resistance state remains up to small negative values of the field. Further increase of the negative magnetic field leads again to consecutive reversal of the particles' magnetic moments accompanied by the switching of the total magnetic moment. The effective exchange field becomes large again and quenches superconductivity. This gives rise to the increase of the resistance. The same measurements performed at a higher temperature (Fig. 2(b,d)) show that the critical fields corresponding to the reversal of the superparamagnetic particles progressively disappear, showing the transition to the unblocked state.

We can draw two important conclusions from the measurements performed on this series of samples. First, strength of the exchange coupling between Al and EuS can be tuned in a broad range of values (see Table 1). And second, the coupling in the Al/EuS system can be so strong that it quenches superconductivity of Al. In this latter case morphology of the EuS layer plays a crucial role allowing for reduced effective magnetic moment due to competing dipolar and exchange interactions between the superparamagnetic grains comprising the polycrystalline film. Further investigations revealed that effective exchange coupling field $\overline{h}$ and the spin-flip relaxation rate τ_{sf} varies with stoichiometry of the EuS layer. We made a series of polycrystalline EuS films and performed analysis of their chemical composition using XPS spectrometer connected to the growth chamber. It turns out that sublimation of the stoichiometric EuS powder at different temperatures gives rise to strong variation of the Eu/S ratio in the films. Results of this study will be published elsewhere, therefore we do not include the data in the current report but this work was crucial to find optimal parameters of the growth of the Al/EuS bilayers.

Having achieved the goal of fabricating samples with a sizable spin-splitting at zero field we then focused on the fabrication of tunneling junctions capable of achieving the spin-polarized tunneling. Previous measurements performed by the Pisa group, reported in the deliverable D2.1, showed that the Cu/EuS/Al junctions fabricated by Moodera have extremely large tunneling barrier resistances. It makes them incompatible with the measuring set-up (resistance of the Vpreamp is too low) and does not allow for a simple measurement of the thermoelectric effect. Moreover, the non-local heating measurements show a net heating of the device without a visible thermal gradient across the junction. These two evidences, together with the fact that the COVID-19 pandemic has restricted our access to the laboratory for many months, has led us to take the decision to focus our efforts on the optimization of the junctions with Co/AlO_x/Al/EuS architecture instead of Cu/EuS/Al.

This project has received funding from the European Union's Horizon 2020 research and innovation programme under grant agreement No 800923.

Thus, we have fabricated a series of Co/AlO_x/Al/EuS devices with a variable thickness of the Al layer. Schematic representation of the device layout and a picture of the devices are shown in the Figure 3(c-d). Superconducting aluminum layer is in contact to 12 nm of EuS which provides the exchange coupling needed for the splitting of the DOS. The spin-dependent tunneling is provided by top 10 nm thick cobalt electrodes. Single Co wire was grown under the same conditions on a separate non-magnetic substrate and its magnetic properties were measured in a VSM magnetometer. Magnetization loops acquired at different temperature in the magnetic field applied along the wire are shown in the Figure 3(b). Squared shape of the loops and large value of the remanent magnetization implies that a strong shape magnetic anisotropy keeps magnetic moment aligned parallel to the wire. At the same time, relatively low coercive field is an indication that the magnetization reversal is concerned with formation and propagation of the domain walls that is expected behaviour for the 200 μm wide stripe. Tunneling conductance presented in the Figure 3(a) demonstrates characteristic asymmetry that proves spin polarization of the junction, as well as a splitting of the conductance peaks reveals the exchange coupling between the Al and EuS.

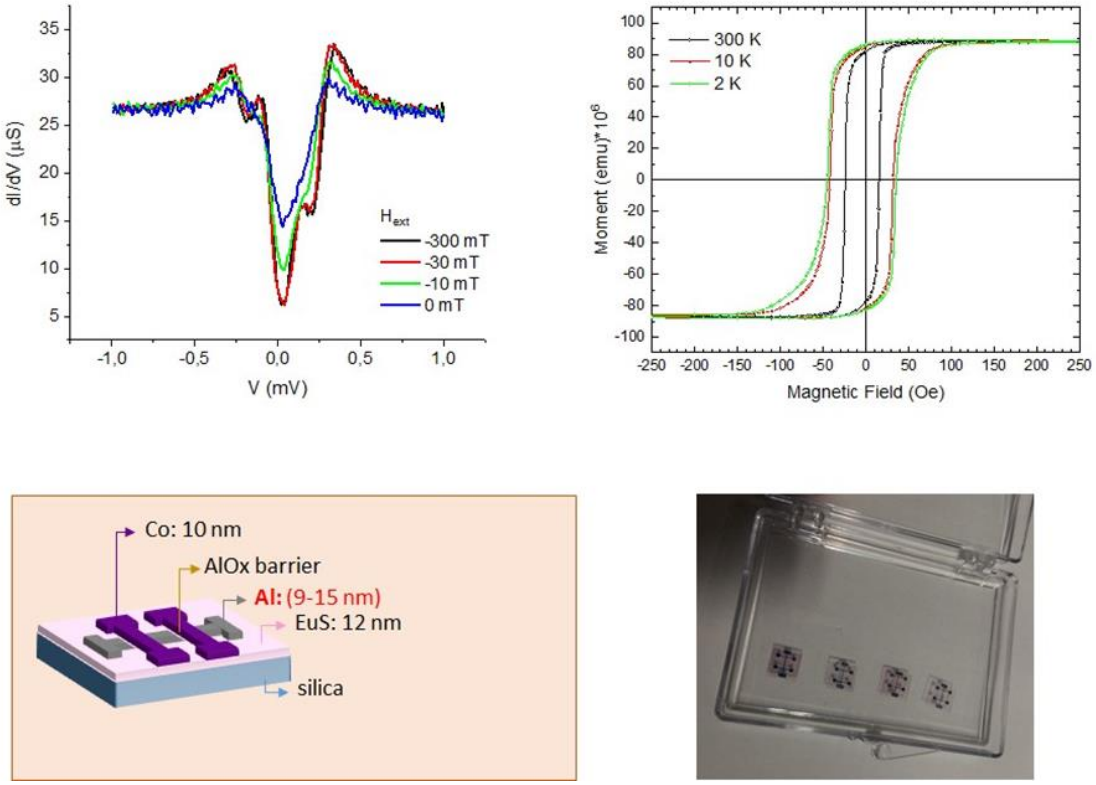

Figure 3: *(a) Tunneling conductance of the Co/AlO_x/Al 12nm/EuS device measured at 30 mK in different magnetic fields. (b) Magnetization loop measured for cobalt wires grown on separate non-magnetic sub- strates. (c) Schematics of the spin-polarized tunneling devices (d) Photo of the Co/AlO_x/Al/EuS devices used in this experiment.*

Contrasting the measured *dI/dV* with our theoretical model we can extract values of the spin-splitting of around 80 μeV and a spin-polarization of 40 − 50%. These values for the

This project has received funding from the European Union's Horizon 2020 research and innovation programme under grant agreement No 800923.

splitting and polarization are of the same order as those obtained from the fitting of the *dI/dV* obtained in Moodera's samples made of Cu/EuS/Al and reported in deliverable D 2.1. Therefore, for the purposes of the SUPERTED detector our $Co/AlO_x/Al/EuS$ junctions are as good as the Cu/EuS/Al junctions. Taking into account that the resistance of the standard AlO_x barrier can be reduced down to $k\Omega$ range for the junctions of the relevant size, we believe that our devices are suitable for building a proof-of-principle thermoelectric element.

Further steps towards demonstration of the thermoelectric effect require post-processing of the $Co/AlO_x/Al/EuS$ junctions aimed to making the heating elements, antennas or absorbers. This as well as reducing of the junctions' area for the investigation of the size effects depend on the lithography. First attempts of patterning performed by the Pisa's group unveiled that originally used fused silica substrates cause difficulties because of the charge accumulation. Therefore, the CSIC group has modified the growth process to use a SiO_2 covered silicon wafers as substrates. First series of the $Co/AlO_x/Al/EuS/SiO_2/Si$ tunneling devices is shipped to the Pisa and Jyväskylä partners for the post-processing.

This project has received funding from the European Union's Horizon 2020 research and innovation programme under grant agreement No 800923.

3. Fabrication of spin-filtering tunnel barriers and searching for alternative magnetic materials

As it was mentioned in the previous sections, the initial proposal of using EuS as a spin-filtering material was evaluated using a series of Cu/EuS/Al samples provided by Dr. Moodera. Measurements performed by the Pisa's group and reported in the deliverable 2.1 showed that the thickness of the EuS barrier has to be in order of a few nm to provide a polarization of 50 %. With this thickness the resistance of the relatively large junctions (250x250 μm^2) was in the order of $G\Omega s$ that is far beyond the range suitable for the applications. Nevertheless, using of magnetic tunnel barriers potentially may provide higher values of spin polarization than what we have already obtained in the Co/AlO_x/Al/EuS junctions with one FM wire. Therefore, we were searching for alternatives to EuS as a material for spin-filtering magnetic barriers. There were few recent works concerned with using of Van der Waals layered magnetic compounds in the tunneling junctions [6, 7, 8]. The advantage of these materials is their propensity for continuous layer-by-layer growth with low density of defects. Together with good dielectric properties it makes layered magnetic compounds good candidates for using in spin-filtering barriers.

We have chosen $NiBr_2$ and $FeBr_2$ that belong to the broad family of the Transition Metal Dihalides layered 2D materials [9]. Bulk $NiBr_2$ and $FeBr_2$ are semiconductors, maintaining their semiconducting behaviour also in the monolayer case [10, 11]. A single slab of these compounds consists of a metal plane embedded between two Br-planes, with a lattice constant of the order of 3.5 Å [10, 11]. Magnetic moments are ordered ferromagnetically within each slab, meanwhile the slabs are coupled antiferromagnetically showing a net magnetic moment of 2.1 μB /at and 3.9 μB /at, respectively. Curie temperature (T_C) was found to be of 52 K for $NiBr_2$ and of 14 K for $FeBr_2$. The band gap is around 4 eV. Although $NiBr_2$ and $FeBr_2$ are antiferromagnets the interslab coupling is weak and a moderate magnetic field is capable of triggering metamagnetic phase transition. Therefore, we will be able to test the spin filtering properties of these materials both in FM and AFM regime.

During the past year we have studied the growth mode, electronic and magnetic properties of thin $NiBr_2$ and $FeBr_2$ films prepared on different substrates. Since these results will be published soon, here we do not include details of the investigations but provide only the conclusions. We have developed a recipe of growth of the stoichiometric $NiBr_2$ and $FeBr_2$ films that does not require Molecular Beam Epitaxy (MBE). Subsequently we have explored them by means of multiple surface science techniques: scanning-tunneling microscopy (STM), scanning-tunneling spectroscopy (STS), X-ray photoemission spectroscopy (XPS), low-energy electron diffraction (LEED), and Angle resolved Ultraviolet Photoemision

This project has received funding from the European Union's Horizon 2020 research and innovation programme under grant agreement No 800923.

Spectroscopy (ARPES). Within this approach we have determined the layer structure when the compounds are grown on metallic substrates and confirmed a layer by layer growth mode. Electronic and magnetic properties studied down to a single slab thickness look suitable for using both $NiBr_2$ and $FeBr_2$ as materials for the magnetic tunneling barriers. Therefore, Al/$NiBr_2$/Al/EuS and Al/$FeBr_2$/Al/EuS junctions will be prepared and sent to our partners for evaluation of the spin filtering performance.

Initial proposal of the SuperTED project included a task of investigation of the spin-split DOS in bilayers of Al/GdN and Al/MnSe. It was left mainly as a backup plan to substitute EuS if the main candidate Al/EuS was impossible to reproduce. Since CSIC group has demonstrated successful growth recipe and managed to produce Al/EuS-based tunnel junction, a search of the EuS substitution turned out to have less priority. Furthermore, the growth of GdN implies a strong experimental development that includes the installations of a new N plasma source, and requires the modification of our actual experimental set-up. This is something that we are still planning to do but, due to the COVID 19 situation, we have seen drastically reduced our in-lab working capability (in 2020 we had severe restrictions to access the laboratories) and thus we decided to postpone the exploration of the alternative materials until the last year of the project.

This project has received funding from the European Union's Horizon 2020 research and innovation programme under grant agreement No 800923.

4. Conclusions

To conclude we summarize here the main achievements for the present WP. We have fabricated and fully characterized the Al/AlO_x/Al/EuS junctions. They show a clear and controllable spin-splitting in the density of states of the Al film adjacent to the EuS, even at zero applied magnetic field. This is a noteworthy achievement considering that until recently only the samples fabricated by Moodera at MIT had exhibited this property. This means that we have achieved the first general goal of the SUPERTED project, developing a fabrication process and setting a European fabrication facility that will allow building devices composed of nanoscale ferromagnetic insulator/superconductor (FI/S) bilayers with an optimized magnetic proximity effect in S. To aid the fabrication process, we also developed theoretical models that allowed us to optimize our samples and in turn provided a full characterization of the devices in terms of effective parameters. Once the spin-splitting in EuS/Al has been controlled, we have coupled such bilayers to a ferromagnetic cobalt film via a tunneling barrier with the goal of observing another main ingredient for SUPERTED detector: a spin-dependent asymmetry of the tunneling current. This was successfully achieved and our samples exhibit spin-polarization efficiencies between 40 and 50 %. Following a feedback of the Pisa group the original silica substrate was changed and the growth recipe was adjusted to produce Co/AlO_x/Al/EuS junctions on SiO_2 covered Si wafers. This modification facilitates the lithography process that is required for the patterning of the heaters, antennas or absorbers. Since we have demonstrated a very good performance of the Al/EuS-based junctions and due to the state of emergency resulting from the COVID-19 pandemic we have decided to postpone investigation of the spin-splitting in the Al/GdN and Al/MnSe-based junctins. Furthermore, we have opted for skipping the growth of the junctions with EuS tunnel barriers. Our decision was based on the fact that the Al/EuS/Cu samples fabricated in the group of Dr. Moodera and measured by the Pisa group showed too high resistances, which hindered the observation of the thermoelectric effect. As alternative materials for the spin-filtering tunneling barriers we have chosen layered magnetic Van der Waals compounds, such as $NiBr_2$ or $FeBr_2$. We have performed investigation of the growth mode of the thin films of $NiBr_2$ and $FeBr_2$ on the relevant substrates. Since their properties compare favorably with the properties of the EuS we foresee successful implementation of these materials as spin-filtering barriers.

4.1 Timetable for the next year

Fabrication of the Co/AlO_x/Al/EuS junctions on SiO_2-covered Si wafers for post processing: patterning of the elements required for the demonstration of the thermoelectric effect and implementation of the detectors.

Growth of the Al/$NiBr_2$/Al/EuS and Al/$FeBr_2$/Al/EuS tunnel junctions to evaluate the spin-filtering performance of the layered magnetic Van der Waals compounds $NiBr_2$ and $FeBr_2$.

Exploration of alternative superconductor materials such as V.

This project has received funding from the European Union's Horizon 2020 research and innovation programme under grant agreement No 800923.

Bibliography

1. MJ Wolf, Christoph Surgers, Gerda Fischer, and D Beckmann. Spin-polarized quasiparticle transport in exchange-split superconducting aluminum on europium sulfide. Physical Review B, 90 (14):144509, 2014.

2. Superted deliverable report 1.1.

3. Alberto Hijano, Stefan Ilic, Mikel Rouco, Carmen Gonzalez Orellana, Maxim Ilyn, Celia Rogero, P. Virtanen, T. T. Heikkila, S. Khorshidian, M. Spies, F. Giazotto, E. Strambini, and F. Sebastian Bergeret. Coexistence of superconductivity and spin-splitting fields in superconductor/ferromagnetic insulator bilayers of arbitrary thickness, 2021.

4. Guo-Xing Miao and Jagadeesh S. Moodera. Controlling magnetic switching properties of eus for con- structing double spin filter magnetic tunnel junctions. Applied Physics Letters, 94(18):182504, 2009.

5. RC O'Hendley. Modern magnetic materials. Modern Magnetic Materials: Principles and Applications (Johns Wiley & Sons, Inc., 2000), 1999.

6. Cheng Gong and Xiang Zhang. Two-dimensional magnetic crystals and emergent heterostructure de- vices. Science, 363(6428), 2019.

7. Daniel C. Ralph Kin Fai Mak, Jie Shan. Probing and controlling magnetic states in 2d layered magnetic materials. Nature Reviews Physics, 1(1), 2019

8. Shi-Jun Liang, Bin Cheng, Xinyi Cui, and Feng Miao. Van der Waals heterostructures for high-performance device applications: Challenges and opportunities. Advanced Materials, 32(27):1903800, 2020.

9. Michael A. McGuire. Crystal and magnetic structures in layered, transition metal dihalides and tri- halides. Crystals, 7(5), 2017.

10. Muhammad Mushtaq, Yungang Zhou, and Xia Xiang. Nix 2 (x = cl and br) sheets as promising spin materials: a first-principles study. RSC Advances, 7(36):22541–22547, 2017.

11. Min Lu, Qiushi Yao, Chuanyun Xiao, Chengxi Huang, and Erjun Kan. Mechanical, electronic, and magnetic properties of nix2 (x = cl, br, i) layers. ACS omega, 4(3):5714–5721, 2019.

This project has received funding from the European Union's Horizon 2020 research and innovation programme under grant agreement No 800923.